

# EXPERIMENT TO DEMONSTRATE ACCELERATION IN OPTICAL PHOTONIC BANDGAP STRUCTURES\*

R.J. England<sup>†</sup>, E.R. Colby, R. Laouar, C.M. McGuinness, D. Mendez, C.-K. Ng, J.S.T. Ng, R.J. Noble, E. Peralta, K. Soong, J.E. Spencer, D. Walz, Z. Wu, D. Xu  
SLAC National Accelerator Laboratory, Menlo Park, CA 94025, USA

## Abstract

Optical scale dielectric structures offer a promising medium for high-gradient, compact, low-cost acceleration of charged particles. An experimental program is underway at the SLAC E163 facility to demonstrate acceleration in photonic bandgap structures driven by short laser pulses. We present initial experimental results, discuss structure and experimental design, and present first estimates of achievable gradient.

## INTRODUCTION

In the drive to achieve beam energies in the TeV range and beyond, it is critical to develop new technologies for particle acceleration which combine higher gradient ( $> 200$  MV/m) acceleration with reduced cost. One possibility which has been proposed in recent years is the use of micron-scale dielectric structures driven by lasers operating in the optical to near infrared regime [1, 2, 3]. The use of a laser as the drive source for the accelerating field offers several benefits, including the high repetition rates ( $> 10$  MHz) and strong electric fields ( $> 0.5$  GV/m) which modern lasers can provide, combined with improved commercial availability and cost when compared with microwave sources. The use of dielectric structures circumvents the problem of power loss in metallic cavities at optical frequencies; it also allows for much larger accelerating gradients due to the higher breakdown thresholds (1-5 GV/m) of dielectric materials.

Dielectric laser acceleration (DLA) refers to the use of infrared (IR) lasers to accelerate charged particles inside of the waveguide in such a structure. The waveguide acts as both the vacuum channel for the beam and as a confining structure to guide an electromagnetic traveling wave mode. Assuming that the guiding channel's transverse dimensions are of the order of the drive laser wavelength (i.e. 1 to 10 microns) the power coupling efficiency to the particle bunches can in principle be as high as 50%, with optimal efficiency at bunch charges of 1 to 20 fC [4]. In order for successive bunches to sit in the accelerating phase of the wave, the requisite bunch durations are on the attosecond scale with intrabunch spacing equal to the laser wavelength (or an integer multiple thereof). A technique for generating the requisite optically microbunched attosecond scale

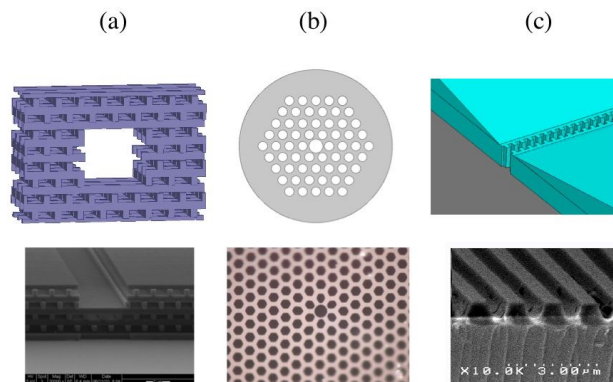


Figure 1: Three dielectric laser accelerator topologies: (a) a 3D silicon photonic crystal structure [7], (b) a hollow-core photonic bandgap fiber [3], and (c) a dual-grating structure [8], showing conceptual illustration (top) and recently fabricated structures (bottom).

beams was recently demonstrated at SLAC [5], and recent work in field emission needle-tip emitters demonstrates that electron beams with the requisite charge and emittance requirements are within reach [6]. As a result of the various technical requirements just mentioned, the beam parameters for an accelerator based on this technology would be quite different from both traditional machines and other advanced schemes.

DLA offers several compelling potential advantages over traditional microwave cavity accelerators. Accelerating gradient is limited by the breakdown threshold for damage of the confining structure in the presence of intense electromagnetic fields. In the DLA scheme operating at typical laser pulse lengths of 0.1 to 1 ps, the laser damage fluences for dielectric materials such as silicon and glass correspond to peak surface electric fields of 400 to 2000 MV/m. This is to be compared with breakdown limits of 40 to 100 MV/m for metal cavities. The corresponding gradient enhancement represents a reduction in active length of the accelerator between 1 and 2 orders of magnitude. Power sources for DLA-based accelerators (lasers) are cheaper than microwave sources (klystrons) for equivalent average power levels due to the wider availability and private sector investment in commercial laser sources. Due to the high laser-to-particle coupling efficiency, required pulse energies are consistent with tabletop microjoule class lasers. Fabrication techniques for constructing three-dimensional dielec-

\*Work supported by U.S. Department of Energy under Grants DE-AC02-76SF00515, DE-FG06-97ER41276

<sup>†</sup> england@slac.stanford.edu

tric structures with nanometer-level precision are well established in the semiconductor industry and the capillary fiber industry. Once a suitable fabrication recipe is developed, on-chip DLA devices with multiple stages of acceleration and waveguides for coupling power to and from the structure could be manufactured at low per-unit cost on silicon wafers.

Several DLA topologies are under investigation, as seen in Fig. 1: (a) a silicon “woodpile” photonic crystal waveguide [7], (b) a glass photonic bandgap (PBG) hollow-core optical fiber [3], and (c) a structure where the beam is accelerated by a transversely incident laser beam in the gap between two gratings [8]. Significant progress has been made in the fabrication of partial or full prototypes of these structures with geometries optimized for accelerator use, as seen in the bottom images. Steps required to make these into working prototypes include alignment and bonding of two of the 9-layer half woodpile structures seen in (a), reducing the fiber dimensions in (b) from an operating wavelength of 7 to 2 microns (where lasers and detectors are more readily available), replacing borosilicate with the more radiation hard silica, and aligning and bonding two of the gratings shown in (c) which are designed for 800nm laser operation. Plans for beam-on demonstrations of one or more of these prototypes and results of recent wakefield testing of several stand-in commercial fibers are discussed below.

## EXPERIMENT OVERVIEW

The E-163 experiment is a multi-phase effort, the ultimate goal of which is to develop custom-built DLA structures, optimized for efficient laser power coupling and high-gradient particle acceleration, into a working accelerator. The first two phases of this plan are illustrated in Fig. 2: (a) a wakefield experiment using commercially available photonic crystal fibers and (b) follow-up acceleration demonstration experiments to be conducted using prototypes of the custom accelerator structures shown in Fig. 1, initially to measure energy modulation in long electron bunches and then net acceleration of a beam that is microbunched at the optical drive laser wavelength. The microbunching scheme, recently demonstrated [5], uses an IFEL interaction followed by a chicane compressor to produce sub-femtosecond microbunches spaced at the laser wavelength.

For the first phase of the experiment in Fig. 2(a), initial results of which are discussed in the following section, wakefield radiation is excited in various commercially available hollow-core photonic crystal fibers. These commercial fibers were designed for use in the telecom industry, and are highly overmoded with poor characteristic impedances, unlike the photonic crystal structures of Fig. 1 that are being designed to support only one or two speed-of-light TM accelerating modes with excellent coupling to the beam and expected gradients ranging from 0.4 to over 1 GV/m. However, in order to successfully excite the desired mode in any of the custom structures of Fig. 1, it is first

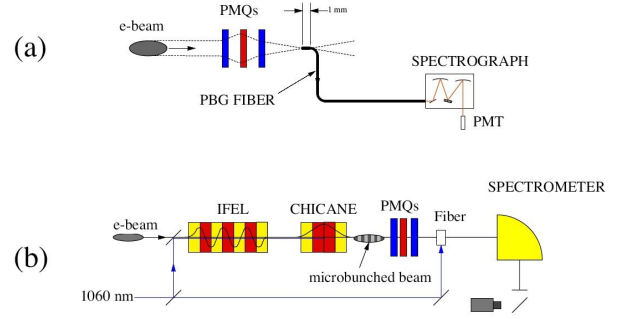


Figure 2: Experimental layouts (not to scale) for the (a) fiber wakefield experiment and (b) follow-up net acceleration experiment.

necessary to identify the mode(s) present and the corresponding wavelengths at speed-of-light (SOL) phase velocity. The commercial fibers are therefore valuable as stand-in devices for developing techniques for exciting and identifying the mode content in the actual accelerator structures once prototypes are available for testing. To our knowledge, electron beam excitation of speed-of-light TM modes in an optical scale photonic crystal waveguide structure has not been previously demonstrated.

The distinction between the commercial fibers used in the presently reported experiment and the high-gradient structures being developed for future testing is highlighted in Fig. 3, which shows simulations of the excited wakefield spectrum for (a) the PBG accelerator in Fig. 1(b) compared with (b) a similar simulation of the commercial HC-800-1 hollow-core optical fiber. The simulation results were obtained using the SLAC in-house time domain code T3P with an axial current excitation and an off-axis field monitor. The spectrum was obtained from the Fourier transform of the time domain response. The geometry of the commercial fiber was carefully modeled based upon scanning electron micrograph images taken at Stanford University. The results predict a single large resonance in the bandgap (highlighted by a blue rectangle) of the custom accelerator structure corresponding to the accelerating mode at a SOL wavelength of 2  $\mu\text{m}$ , to be compared with a highly structured mode content in the bandgap of the commercial fiber. Cartoon illustrations of the bandgap and excited modes (dispersion curves in the bandgap are shown by yellow lines) are presented below each plot in Fig. 3. Spectral content at higher and lower frequencies corresponds to higher order bandgaps, index guided modes related to the outer boundaries and gross geometry of the fiber, and so-called *lattice modes*. The latter are essentially lossy radiation modes that are poorly confined and lie outside the edges of the bandgap. Such modes are unlikely to survive for more than a few tens of wavelengths of longitudinal propagation since they are highly attenuated due to radiative losses. An estimate of the power loss for one representative lattice mode based upon BandSolve simulations

of the commercial fibers was found to be in excess of 200 dB/mm.

For the initial fiber wakefield experiments of Fig. 2(a), a triplet of permanent magnet quadrupoles (PMQs) has been used to focus a 10 to 50 pC beam of 60 MeV electrons generated by the NLCTA photoinjector gun and X-band accelerator into the hollow cores of commercial telecom PBG fibers with bandgaps centered at various optical to IR wavelengths. The fibers are held in an aluminum keeper which constrains them to a 1 mm straight section, followed by a 90 degree turn which bends them out of the beam path on a 3 mm radius. The keeper also incorporates two beam diagnostics: an yttrium aluminum garnet (YAG) profile monitor and a tantalum knife edge for measuring the spot size at the focus of the PMQs. The fibers and the diagnostics can be precisely moved into or out of the beam path by way of an in-vacuum stage assembly with 4-axes of control (x, y, tip, and tilt) and 50 nm spatial resolution. To reduce photon losses, the fiber lengths have been minimized and connectorized feedthroughs have been avoided. The primary losses are therefore due to F-number mismatch, grating efficiency (85%), and the reflectivity of the mirrors (88%) in the spectrograph (Newport model MS-260i), giving an expected monochromatic throughput of 38%, to be compared with a recently measured value of  $40 \pm 5\%$ .

## RECENT EXPERIMENTAL RESULTS

Pursuant to the goals of the broader experimental program discussed in the prior section and illustrated in Fig. 2, wakefield excitation experiments are currently underway as part of the first phase of this effort, using several of the commercial PBG fibers discussed above as stand-ins for future photonic crystal accelerator prototypes that are being developed and are not likely to be available for testing until later this year. In recent experimental runs, beam-induced wakefield radiation has been successfully observed in commercial PBG hollow-core fibers designed for telecom operation at wavelengths of 800, 1060, and 2000 nm. The detector used was a Hamamatsu R5108 photomultiplier tube operating at room temperature. Strong signal was observed when each of the tested fibers was inserted into the beam path with the downstream end imaged directly onto the PMT cathode. A remotely controlled filter wheel was used to verify that the signal was due to optical light from the fibers and not due to x-ray background or electrical noise. Since the excitation is produced by broadband Schottky noise from an electron bunch that is long compared with optical wavelengths, various modes of the fiber may be excited, including TE and TM like modes, as well as higher frequency modes corresponding to additional bandgaps. Since one of the primary goals of this experiment is to develop a technique for rapidly characterizing all of the modes of the structure, a broadband excitation is desirable and experimentally simpler than coherently exciting the fiber with a microbunched beam. The details of this approach and estimates of photon yield and fiber losses

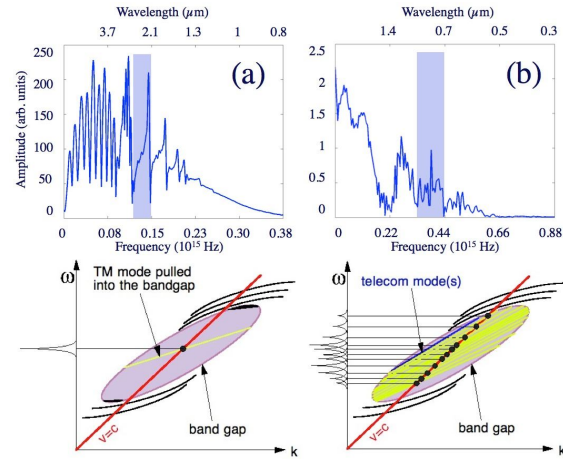


Figure 3: At top: simulations of wakefield spectrum for (a) the single-mode-bandgap high-gradient accelerator design of Fig. 1(b), prototypes of which are being developed; and (b) the highly overmoded but easily obtained HC-800-1 commercial fiber used as a stand-in, with bandgaps highlighted in blue. At bottom: cartoon illustrations of the corresponding bandgap content of the two structures.

have been presented previously [9].

With the spectrograph employed to spectrally analyze the output radiation of the fibers at their respective bandgap centers (800, 1060, 2000nm) a convincing signal was only seen with the 800 nm fiber (Crystal Fibre HC-800-1). This is likely due to the fact that the PMT employed has peak sensitivity at 800nm, with a falloff by an order of magnitude at 1060 nm. Future experiments will use a recently purchased IR photomultiplier tube with a flat response to 1600 nm. The PMT signal was amplified and filtered with a 10Hz high-pass filter and integrated over a 40 ns window spanning the peak of the observed signal. The spectrograph wavelength was then randomly varied at 1 minute intervals, by computer automated rotation of its internal grating, within a range of wavelengths spanning the expected bandgap of the fiber. A fast shutter was used to block and unblock the optical signal at 1Hz in order to distinguish between optical signal and x-ray background, as detector signal was collected at 10Hz.

The resulting data, shown in Fig. 4, has been processed by a rolling average over the 60nm window of the spectrograph. Due to the relatively low spectral resolution of the scan, resonances of individual fiber modes cannot be discerned. However, the width of the bandgap region and the falloff in amplitude near its edges is consistent with detailed simulation results of the TM modes in the fiber.

In addition to the time domain wakefield simulation shown in Fig. 3(b), the modes of the HC-800-1 fiber were simulated using the commercial photonic crystal code BandSolve. The geometry of the lattice and defect region were carefully modeled based upon scanning electron micrograph scans of the fiber. Eigenmodes were simulated over a range of wavenumbers spanning the bandgap region



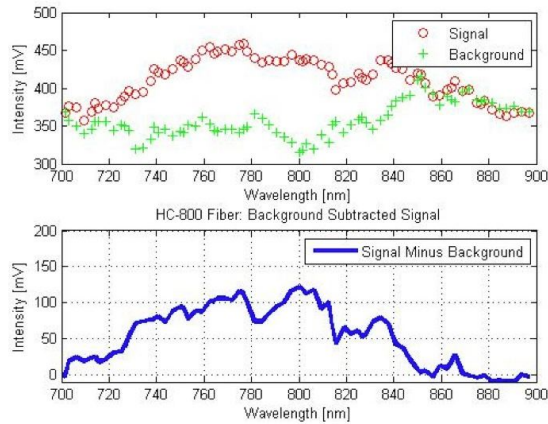


Figure 4: Spectral scan of the wakefield radiation in the HC-800-1 fiber showing averaged signal and background (top) and background subtracted signal (bottom) over the full bandgap region.

in increments of  $0.25/a$ , where  $a = 2.3 \mu\text{m}$  is the photonic lattice pitch. The results predict 38 modes spanning a spectral region from 704 nm to 862 nm, consistent with the data in Fig. 4. A review of the modes closest to the speed of light line at the 18 wavenumber values corresponding to the simulation step size indicates that they are largely TM-like. A detailed reconstruction of the detector signal from these simulations would require identifying all of the modes at SOL phase velocity and calculating their coupling to the longitudinal electric field of the mode as well as computing their power loss ( $dP/dz$ ) in the fiber, an exercise that has not yet been undertaken.

The next experimental run using the commercial telecom fibers will focus on the modes of the HC-1060 fiber, which has been predicted using BandSolve simulations to possess at least two TM modes with high characteristic impedance, corresponding to a maximal accelerating gradient of approximately 30 MV/m operating at damage threshold. Although this is more than an order of magnitude lower than the expected gradient in custom-built accelerator structures, these fibers could be used to develop the needed experimental methods for identifying TM modes in such structures pending completion of the prototypes of Fig. 1. Furthermore, if such a mode is confirmed, the fiber could be used as an initial test structure for acceleration demonstration experiments. In spite of their overabundance of bandgap modes and relatively poor characteristic impedance (at most 1-5 m $\Omega$ ), these off-the-shelf optical fibers offer an inexpensive and available solution for initial testing of photonic crystal accelerator structures.

## CONCLUSIONS

An experiment is underway at the E-163 test beamline at SLAC to use dielectric photonic crystal structures as laser-driven accelerators. As prototypes of three different pro-

posed high-gradient accelerator structures are being fabricated, measurements are underway to test a technique for identifying modes with speed-of-light phase velocity using commercially available hollow-core photonic crystal fibers as stand-ins. The modes of the fibers are excited with a relativistic electron bunch and the Schottky wakefield radiation thereby produced is spectrally analyzed. Initial experimental results, combined with detailed simulations of the fibers, show evidence of successful excitation of TM modes within the bandgap of the HC-800-1 fiber which is centered around 800 nm. This represents the first experimental demonstration of an optical wavelength photonic crystal waveguide operated as an accelerator structure. The next stage of this phase of the experiment will focus on resolving individual modes in the commercial fibers, including a 1060 nm commercial fiber. This effort will be aided by improved shielding of the apparatus to reduce the x-ray background, and by extending the sensitivity and spectral range of the detector.

## REFERENCES

- [1] M. Rosing and W. Gai. Longitudinal and transverse wake field effects in dielectric structures. *Phys. Rev. D*, 42:1829–1834, 1990.
- [2] A. Mizrahi and L. Schachter. Optical Bragg accelerators. *Phys. Rev. E*, 70:016505, 2004.
- [3] X. E. Lin. Photonic band gap fiber accelerator. *Phys. Rev. ST-AB*, 4:051301, 2001.
- [4] R. H. Siemann. Energy efficiency of laser driven, structure based accelerators. *Phys. Rev. ST-AB*, 7:061303, 2004.
- [5] C. M. S. Sears and et al. Production and characterization of attosecond electron bunch trains. *Phys. Rev. ST-AB*, 11:061301, 2008.
- [6] P. Hommelhoff, Y. Sortais, A. Aghajani-Talesh, and M. A. Kasevich. Field Emission Tip as a Nanometer Source of Free Electron Femtosecond Pulses. *Phys. Rev. Lett.*, 96:077401, 2006.
- [7] B. M. Cowan. Three-dimensional dielectric photonic crystal structures for laser-driven acceleration. *Phys. Rev. ST-AB*, 11:011301, 2008.
- [8] T. Plettner, P. P. Lu, and R. L. Byer. Proposed few-optical cycle laser-driven particle accelerator structure. *Phys. Rev. ST-AB*, 9:111301, 2006.
- [9] R. J. England, E. R. Colby, R. Ischebeck, C.M. McGuinness, R. Noble, T. Plettner, C. M. S. Sears, R. H. Siemann, J. E. Spencer, and D. Walz. Experiment to detect accelerating modes in a photonic bandgap fiber. In *13th Advanced Accelerator Concepts Workshop*, volume 1086 of *AIP Conference Proceedings*, pages 550–555, Santa Cruz, CA, 2008.